DIAMOND PIN THERMAL NEUTRON DETECTORS

Holmes[1‡], J., Brown[1], J., Koeck[1], F. A., Johnson[1], H., Benipal[2], M. K., Zaniewski[1], A., Alarcon[1*], R., Goodnick[3], S. M., and Nemanich[1], R. J.

[1]Department of Physics, Arizona State University, Tempe, AZ 85287-1504, United States of America
[‡]Phynix Technologies LLC, Scottsdale, Arizona, United States of America
[2]ADVENT Diamond Inc., Scottsdale, Arizona, United States of America
[3]School Of Electrical, Computer and Energy Engineering, Arizona State University, Tempe, AZ 85287-9309, United States of America

Abstract

Diamond PIN diodes with an approximately 5-μm thick i-layer and coated with a thin boron nitride (BN) layer have been tested with a thermal neutron beam flux of 4.4×10^6 n/s/cm². Pulse height spectra showed features associated with α and ^{7}Li fission products, consistent with the thickness of the BN layer. An irradiation test with a 1 MeV neutron equivalent fluence of 10^{15} n/cm² showed no significant alteration in the count rate of the tested detector.

Resumen

Diodos PIN de diamante con una i-capa de aproximadamente 5-μm de grosor y recubiertos con una fina capa de nitrato de boro han sido probados con un flujo de neutrones de 4.4×10^6 n/s/cm². La detección de neutrones se demuestra en el espectro de altura de pulso a través de los productos de fisión α and ^{7}Li, consistentes con el grosor de la capa de nitruro de boro. Una prueba de irradiación con una fluencia equivalente de neutrones de 1 MeV de 10^{15} n/cm² no alteró de manera significativa la tasa de conteo del detector probado.

I.   INTRODUCTION

Diamond has very promising properties for a radiation detector and diamond detectors under α-particle irradiation have shown 100% charge collection efficiency with an energy resolution < 1% (Kaneko et al., 2006). The properties of diamond that contribute to its value in radiation detection include wide bandgap (5.5 eV), high electron and hole mobilities, high breakdown field, and high displacement damage threshold. These properties combine to enable radiation hard, low background, relatively efficient particle detectors. We have developed and demonstrated diamond p-i-n (PIN) diode particle detectors based on epitaxial growth of n-type, phosphorus doped diamond, high purity undoped (intrinsic) diamond, and p-type, boron doped diamond (Holmes et al., 2018). The detector i-layer thickness has been adjusted to match the penetration depth of designated α-particles, which minimizes background due to gamma radiation and high energy particles. Moreover, the detectors can be operated in pulse mode with a bias of only a few volts. The unique properties of the p-i-n diode led to the development of a new method to mitigate the polarization effect (Holmes et al., 2019).

The conversion of thermal neutrons into directly detectable particles is best accomplished with the ^{10}B(n,α) reaction (Knoll, 2010). The reaction products are emitted in exactly opposite directions, sharing the energy always in the same manner such that for the 94% branching ratio $E_{Li} = 0.84\ MeV$ and $E_\alpha = 1.47\ MeV$.

Building on the results previously obtained with a p-i-n diamond detector (Holmes et al., 2018), where α-detection was accomplished with no significant background and with minimal sensitivity to gamma radiation, this paper reproduces and summarizes the results obtained from tests of thermal neutron detectors developed through the integration of a boron nitride (BN) neutron absorption layer and an

[1*]Corresponding Author: ricardo.alarcon@asu.edu

optimized diamond p-i-n detector (Holmes at al., 2020). Like diamond, boron nitride is a hard, high temperature material that is expected to survive in extreme environments.

A number of BN/diamond PIN neutron detectors have been fabricated at Arizona State University and tested with consistent results at The Ohio State University Nuclear Reactor Laboratory (OSU-NRL). The tests include pulse counting measurements at a thermal neutron beamline with a flux of 4.4×10^6 n/cm^2/s and irradiation of the detectors in the reactor core to a 1-MeV neutron equivalent fluence of 10^{15} n/cm^2.

II.   MATERIALS AND METHODS

A schematic of the complete detector is shown in Figure 1. The PIN detector diodes were prepared using 3mm x 3mm x 0.3mm high-pressure, high-temperature (HPHT), boron doped substrates with a boron concentration of $\sim 1.2 \times 10^{20}$ cm^{-3}. With a crystallographic (111) orientation and minimum miscut angle of ± 1.5 deg, the surface was polished to an RMS roughness of ~ 40 nm. The growth of the diamond PIN substrate and the deposition of the electric contacts have been described in previous papers (Holmes et al., 2018, 2020). The BN layer was deposited on top of the electrical contacts using an electron cyclotron resonance (ECR) microwave plasma chemical vapor deposition (ECR MP CVD).

The thickness of the BN conversion layer is limited by the range of the 1.47 MeV α-particle (4.25 μm) and the growth rates for BN by standard methods such as sputtering were too slow for practical device fabrication. The growth mechanism proposed in prior studies (Zhang et al., 2007; Shammas et al., 2015), suggested the active growth species of BN is BF$_x$ and NH$_x$. We found that increasing the flow of BF$_3$ and H$_2$ the reaction will shift toward the products and increase the growth rate.

To determine the growth rate, we used p-type silicon wafers with the same titanium, platinum, gold structure on the surface to mimic the contact pad of the detectors. Both *in-situ* X-ray photoelectron spectroscopy and *ex-situ* ellipsometry (Jablonski & Zemek, 2009) were used to measure a growth rate of 3.7 ± 0.7 nm/min. A BN layer of 445 ± 89 nm was deposited on the sample that underwent the thermal neutron beam and irradiation tests first reported in (Holmes et al., 2020).

After BN deposition, silver epoxy was used to make electrical contact and adhere the back side of the detector to a printed circuit board. A nano-milling process utilizing an atomic force microscope (AFM) with a single crystal diamond tip was employed to remove a 90x180 μm^2 area of BN and expose the gold contact below. Finally, gold wires were utilized to wire bond from this exposed contact pad to the printed circuit board.

Figure 1
Detector Schematic
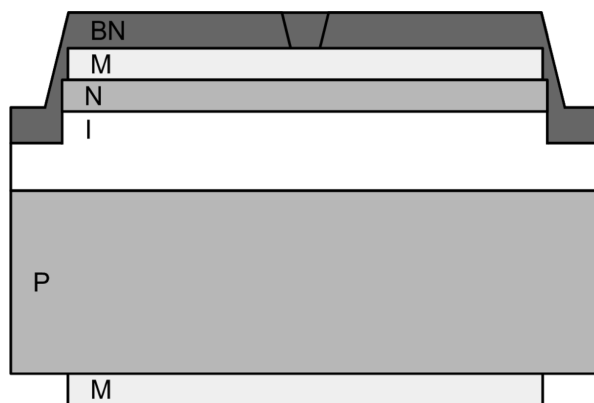
Note: A cross-sectional view of the detector (not at scale) showing the layers labeled *BN*: boron nitride layer, *M*: Ti/Pt/Au contacts, *N*: n-type (P-doped) diamond, I; intrinsic diamond, and *P*: p-type (B-doped) diamond.

Measurements were carried out using a thermal neutron beamline at the 500 kWth research reactor facility at OSU-NRL. The beamline delivers a thermal equivalent neutron flux of 4.4×10^6 n/s/cm^2, with a circular beam size of 3-cm diameter, when reactor is operated at 450 kWth. The detectors were read out using an ORTEC-based pulse counting electronics system. The signal connection was fed into an ORTEC 142A preamplifier and the output connected to an ORTEC 672 spectroscopy amplifier. The n-side of the diamond diode was biased between -3 V and 45 V relative to the p-side (reverse bias is positive) using the ORTEC 428 detector bias supply. The p-side was biased to ground, and the response to the neutron induced reaction products from the BN layer was measured from the n-side.

III.   RESULTS AND DISCUSSION

Figure 2 shows the pulse height distribution obtained with a diamond diode that was coated with a BN layer approximately 0.5 µm thickness. The two most prominent peaks (around channels 35 and 85 respectively) correspond to the 94% branching ratio of the ^{10}B(n,α)^{7}Li capture reaction. This reaction releases a ^{7}Li nuclei with a kinetic energy of 0.84 MeV in coincidence with a 1.47 MeV α-particle. The peak observed around channel 105 corresponds to the 1.78 MeV α-particle from the 6% branching ratio, while the accompanying ^{7}Li nuclei with a kinetic energy of 1.01 MeV contribute the background curve centered around channel 50.

In the low channel region, 584 keV protons from the ^{14}N(n,p)^{14}C reaction insignificantly contribute to the signal due to self-absorption and the low ^{14}N neutron capture cross-section (1.83 barn for thermal neutrons) comparted to ^{10}B neutron capture (3842 barn for thermal neutrons). The decay products of the ^{10}B(n,α)^{7}Li reaction experience a partial loss of kinetic energy while travesing through a portion of the 0.5 µm BN layer. After correcting for this energy loss, the identifiable peaks in Figure 2 exhibit a linear relation with a slope of $15.0^{+2.5}_{-1.6}$ keV/channel (95% confidence interval). These measurements indicate that the tested detector can operate in pulse counting mode up to fluxes of 10^9 n/s/cm^2, considering the present data acquisition capabilities of 160k counts per second. However, this count rate limit can be extended by approximately two orders of magnitude using faster amplifiers and digitizers that are readily available.

Figure 2
Pulse Height Distribution
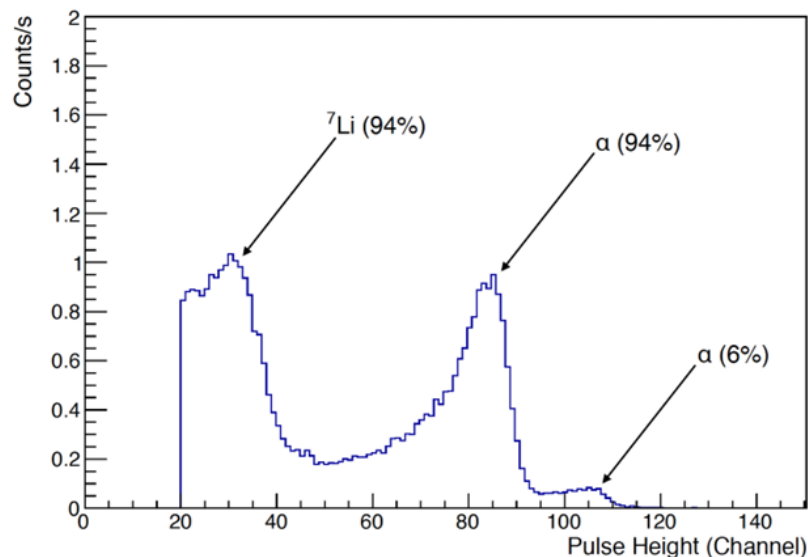
Note: The horizontal axis is the charge collected per pulse and the vertical axis is the count rate for a detector in front of the 4.4×10^6 n/s/cm^2 thermal neutron beam. The arrows show the detection of the α and ^{7}Li particles from the 94% branching ratio and the α particle from the 6% branching ratio.

An irradiation test was conducted, subjecting the detector to a 1 MeV neutron equivalent fluence of 10^15 n/cm^2. After a cooldown period, the detector was handled to enable a measurement of its pulse height distribution at the thermal neutron beamline under identical conditions as those used to obtain the results shown in Figure 2. The results are presented in Figure 3, with the curves representing the pre-irradiation and post-irradiation results. The count rates beyond the threshold are very similar in both curves, indicating no significant change in this aspect. However, the pulse height distribution in the post-irradiation curve is shifted towards lower values by an estimated amount of approximately 250 keV. Despite this shift, the charge collection efficiency remains largely unaffected (Holmes et al., 2020). The underlying cause of this shift is currently under investigation for further understanding.

Figure 2
Irradiation Effect
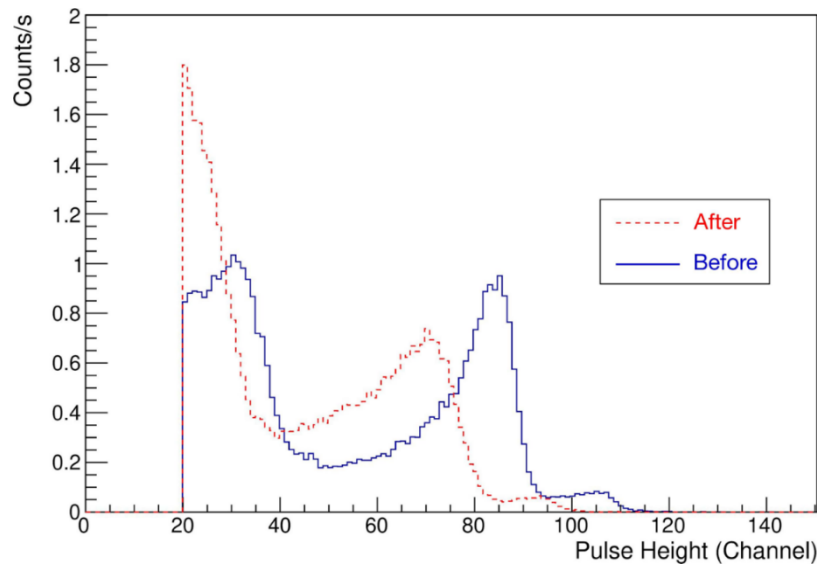
Note: The pulse height distribution for the detector in front of the thermal neutron beam before (solid line) and after (dashed line) irradiation by a 10^{15} n/cm^2 fluence.

II. REFERENCES

Holmes, J., Dutta, M., Koeck, F., Benipal, M., Brown, J., Fox, B., Hathwar, R., Johnson, H., Malakoutian, M., Saremi, M., Zaniewski, A., Alarcon, R., Chowdhury, S., Goodnick, S., & Nemanich, R. (2018). A 4.5 μm PIN diamond diode for detecting slow neutrons. *Nuclear Inst. and Methods in Physics Research, A 903*, 297.

Holmes, J., Dutta, M., Koeck, F., Benipal, M., Hathwar, R., Brown, J., Fox, B., Johnson, H., Zaniewski, A., Alarcon, R., Chowdhury, S., Goodnick, S., & Nemanich, R. (2019). Neutralizing the polarization effect of diamond diode detectors using periodic forward bias pulses. *Diamond and Related Materials 94*, 162.

Holmes, J., Brown, J., Koeck, F. A., Johnson, H., Benipal, M. K., Kandlakunta, P., Zaniewski, A., Alarcon, R., Cao, R., Goodnick, S. M., & Nemanich, R. J. (2020). Performance of 5-μm PIN diamond diodes as thermal neutron detectors. *Nuclear Inst. and Methods in Physics Research, A 961*, 163601.

Jablonski A., & Zemek J. (2009), Surface and Interface Analysis 41, 193–204.

Kaneko, J.H., Tanaka, T., Imai, T., Tanimura, Y., Katagiri, M., Nishitani, T., Takeuchi, H., Sawamura, Y., & Iida, T. (2003). Radiation detector made of a diamond single crystal grown by a chemical vapor deposition method. *Nuclear Inst. and Methods in Physics Research, A 505,* 187. Knoll

Knoll, G.F., 2010. Radiation Detection and Measurement, John Wiley, Hoboken, N.J.

Shammas, J., Sun, T., Koeck, F. A. M., Rezikyan, A. & Nemanich, R. J. (2015). In situ photoelectron spectroscopic characterization of c-BN films deposited via plasma enhanced chemical vapor deposition employing fluorine chemistry. *Diamond and Related Materials 56*, 13.

Zhang, W. J., Chong, Y. M., Bello, I. & Lee, S. T., (2007). Nucleation, growth and characterization of cubic boron nitride (cBN) films. *Journal of Physics D: Applied Physics 40*, 6159.

Acknowledgment: